Stone–Wales Defects in Single-Walled Boron Nitride Nanotubes: Formation Energies, Electronic Structures, and Reactivity

ARTICLE *in* THE JOURNAL OF PHYSICAL CHEMISTRY C · JANUARY 2008

Impact Factor: 4.77 · DOI: 10.1021/jp077115a

Stone−Wales Defects in Single-Walled Boron Nitride Nanotubes: Formation Energies, Electronic Structures, and Reactivity

Yafei Li,[†] Zhen Zhou,*[,†] Dmitri Golberg,[‡] Yoshio Bando,[‡] Paul von Ragué Schleyer,[§] and Zhongfang Chen*[,‡,§]

Institute of New Energy Material Chemistry, Institute of Scientific Computing, Nankai University, Tianjin 300071, People's Republic of China, International Center for Young Scientists, National Institute of Materials Science, Namiki 1-1, Tsukuba, Ibaraki 305-0044, Japan, and Department of Chemistry and Center for Computational Chemistry, University of Georgia, Athens, Georgia 30602

Received: September 4, 2007; In Final Form: October 22, 2007

The geometries, formation energies, electronic properties, and reactivities of Stone−Wales (SW) defects in single-walled (8,0) boron nitride nanotubes (BNNTs) were investigated by means of gradient-corrected density functional theory (DFT) computations. SW defects deform BNNTs severely and result in local curvature changes at defect sites. The energies of defect formation increase with increasing tube diameters and are orientation dependent. Depending on the SW defect orientations, additions to central 7-7 ring fusions can be either more or less favorable than to defect-free sites. The reaction energies of model H_2 addition are mostly endothermic for defective as well as pristine BNNTs, but reactions at the most favorable sites near SW defect (homoelement N−N bonds followed by the B−B bond sites) are exothermic. This and the fact that the band structures of BNNTs are only slightly changed by SW and vacancy defects as well as by chemical additions at low modification ratios endow BNNTs with great application potential.

1. Introduction

Boron nitride nanotubes (BNNTs),[1] theoretically proposed in 1994[2] and first synthesized in 1995,[3] offer some important advantages over their close cousins, the single-walled carbon nanotubes (CNTs). While such CNTs can be either metallic or semiconducting, depending on the tube chiralities and diameters, all BNNTs are wide band gap semiconductors. Their ∼5.5-eV band gaps are weakly dependent on tube diameters, helicity, and wall numbers.[2] Moreover, BNNTs resist oxidation more than CNTs.[4] The uniform electronic properties and relative chemical inertness of BNNTs promise many applications in nanotechnology, such as force sensors,[5] hydrogen storage media,[6] and nanocable sheaths.[7] Moreover, many experimental and theoretical studies were performed to tune the electronic properties of BNNTs in order to widen their potential applications.[8−10]

The experimentally available BNNTs are not perfect. Vacancies, antisites (an atom occupying the site of another one), pentagons, heptagons, dopants, and Stone−Wales (SW) defects[11] may impact the properties of BNNTs vitally and alter their band structures.[12,13] Despite this, available theoretical studies mainly focus on perfect BNNTs; the effects of defects have hardly been investigated.[6h,12−15]

SW 5-7-7-5 ring defects are very important in CNTs and BNNTs. Their presence has been established unambiguously in CNTs and BNNTs spectroscopically.[16] Earlier studies of SW defects in CNTs[17−21] revealed interesting metal and gas adsorption,[16] chemical reactivity,[20] and mechnical properties.[21] However, detailed studies of SW defects in BNNTs are rather scarce. Bettinger et al. reported that 5-7-7-5 arrangements, despite having homoelemental B−B and N−N bonds, are more favorable than the 4-8-8-4 alternatives.[15] Wu et al.[6h] found that SW and other defects can enhance H_2 adsorption (but only the central 7-7 ring fusion was considered for SW defect); some defects such as boron antisite, carbon-substituted nitrogen site, and vacancies can even dissociate H_2 on BNNTs. Very recently, using cluster models, An et al.[22] examined the adsorption of a number of species relevant to chemical gas sensors (such as H, O, CO, H_2, and NH_3) with BNNTs and investigated the sidewall reactivity of SW defects in BNNTs. Many questions are still unanswered. Are smaller diameter BNNTs more favorable for SW defect formation? Does the orientation of SW defects affect the electronic properties? What is the most reactive site in SW defective BNNTs? In this paper, periodic boundary density functional theory (DFT) computations were performed to address these questions.

2. Computational Methods

Since BNNTs adopt a preferential zigzag orientation during growth,[23] a series of zigzag models were selected in our study. The thermochemistry of H_2 additions to pristine BNNTs and SW defect sites were evaluated as a measure of relative reactivity.

DFT computations employed the plane-wave pseudopotential technique implemented in the Vienna ab initio simulation package (VASP).[24] The generalized gradient approximation (GGA) with the PW91 functional[25] and a 360-eV cutoff for the plane-wave basis set were adopted in all the computations. The electron−ion interactions were modeled by the ultrasoft pseudopotentials.[26] One-dimensional (1-D) periodic boundary condition (PBC) was applied along the tube axis in order to simulate infinitely long nanotube systems. Interactions between SW

* To whom correspondence should be addressed. E-mail: zhouzhen@nankai.edu.cn (Z.Z.); chen@chem.uga.edu (Z.C.).
[†] Nankai University.
[‡] National Institute of Materials Science.
[§] University of Georgia.

10.1021/jp077115a CCC: $40.75
Published on Web 01/11/2008

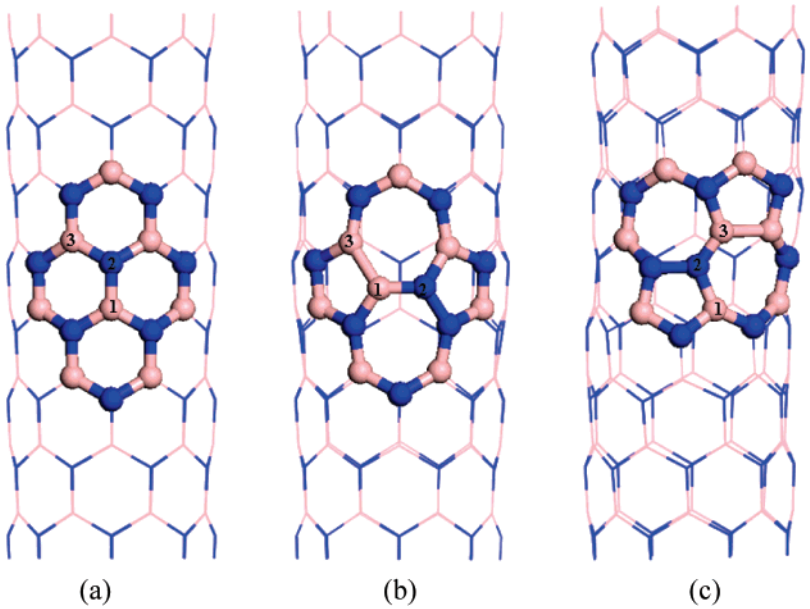

Figure 1. Structures of perfect and defective tubes: (a) perfect (8,0) BNNT, (b) (8,0)-I, (c) (8,0)-II. The B and N atoms are represented in orange and blue, respectively. The SW defects are highlighted in ball−stick representations in (b) and (c) to emphasize their differences from the pyrene-like structures in (a).

defects and their 1-D periodic images were avoided in our computational supercell models, which include four unit cells of zigzag tubes (for example, supercell length $c = 17.26$ Å for a (8,0) BNNT). Five k points were used for sampling the 1-D Brillouin zone, and the convergence threshold was set as 10^{-4} eV in energy and 10^{-3} eV/Å in force. The positions of all the atoms in the supercell were fully relaxed during the geometry optimizations. On the basis of the equilibrium structures, 21 k points were then used to compute band structures. For comparison, the hexagonal BN sheet using a 6×6 supercell on the graphene plane with a SW defect was studied as well.

Rotating a B−N bond by 90° in the BN hexagonal network of BNNTs (Figure 1a) results in SW defects. There are two kinds of B−N bonds in zigzag BNNTs due to local curvatures (denoted by B1−N2 and N2−B3 in Figure 1a). Consequently, two types of SW defects for each BNNT (labeled as (n,0)-I and (n,0)-II) are possible. The former is obtained by rotating the B1−N2 bond parallel to tube axis (Figure 1b), while the latter is obtained by rotating a slanted N2−B3 bond (Figure 1c).

Defect formation energies (the energies required to form SW defects) are defined as: $E_F = E_{SW} - E_{perfect}$, where E_{SW} and $E_{perfect}$ are the total energy of the BNNT containing a SW defect and that of the perfect BNNT, respectively. The reaction energies for addition of H_2 molecules are evaluated as: $E_R = [E_{(BNNT-2H)} - E_{BNNT} - E_{H2}]$, where $E_{(BNNT-2H)}$, E_{BNNT}, and E_{H2} stand for the total energy of the H_2-added BNNT, the pristine BNNT, and the H_2 molecule, respectively.

3. Results and Discussion

3.1. Local Structures of SW Defects in (8,0) BNNTs. The local structures of the two kinds of SW defects in (8,0) BNNTs are compared with those of perfect nanotubes in Table 1. The pyramidalization angle (Θ_P) is a measure of the degree of sp^3 hybridization of an atom, defined as ($\theta_{\sigma\pi} - 90°$), where $\theta_{\sigma\pi}$ is the angle between σ and π bonds.[27]

The structural deformation due to the formation of SW defects is more severe for (8,0)-II than for (8,0)-I (Table 1 and Figure 1; the pyramidalization angles of the atoms close to the SW defect site are given in Table S1 in the Supporting Information).

TABLE 1: Bond Lengths (d) of B1−N2 and N2−B3, Pyramidalization Angles (Θp) of the Central B and N Atoms, and Formation Energies (E_F) of SW Defects in Defective Tubes

	d (Å)	Θp (degree)	E_F (eV)
perfect (8,0)	1.441,[a] 1.455[b]	3.81, 9.15	
(8,0)-I	1.414	8.02, 11.1	4.85
(8,0)-II	1.361	6.38, 2.54	5.84

[a] B1−N2 bond. [b] N2−B3 bond (see Figure 1).

Homoelemental B−B and N−N bonds are present in both kinds of defective tubes. The calculated B−B and N−N bond lengths for (8,0)-I are 1.724 and 1.485 Å, respectively, somewhat longer than those for (8,0)-II (1.666 and 1.442 Å, respectively). The formation of B−B and N−N bonds in BNNTs is unfavorable energetically.[16] The B−N bonds at the 7-7 ring fusions of SW defects (1.414 and 1.361 Å in (8,0)-I and (8,0)-II, respectively) are both shorter than the typical B−N bonds in the perfect tube (1.441 and 1.455 Å, respectively). The B and N atoms at the 7-7 ring fusion of SW defects in (8,0)-I move outward from the tube surface, and the curvature-induced Θ_P's of the B and N atoms are 8.02 and 11.1°, respectively. In comparison, in (8,0)-II, the B and N atoms at the 7-7 ring fusion of SW defects move inward to the tube center, and the Θ_P's of the B and N atoms are 6.38 and 2.54°, respectively. The pyramidalization angles of the B and N atoms at the 7-7 ring fusion in (8,0)-I tube are closer to those in a perfect BN tube, the deviations (4.21 and 0.95°) are less pronounced than those in the (8,0)-II tube (2.57 and 6.61°, respectively). Compared with the (8,0)-II alternative, the less deformed (8,0)-I tube is more stable and has smaller defect formation energy, in agreement with An et al.'s finding based on cluster models.[22] These SW defect formation energies depend on the orientation and on Θ_P of the central atoms at the 7-7 ring fusion. Yang et al.[28] have reported similar theoretical results on (10,0) CNTs.

3.2. Energies of Forming SW Defects in BNNTs with Various Diameters. Pan et al. reported that the energies of forming SW defects in single-walled CNTs depend not only on the defect orientations but also on the tube radii.[17] The latter is true for BNNTs as well. We considered both (n,0)-I and (n,0)-II SW defects in a series of zigzag (n,0) (n = 7, 8, 10, 12, or

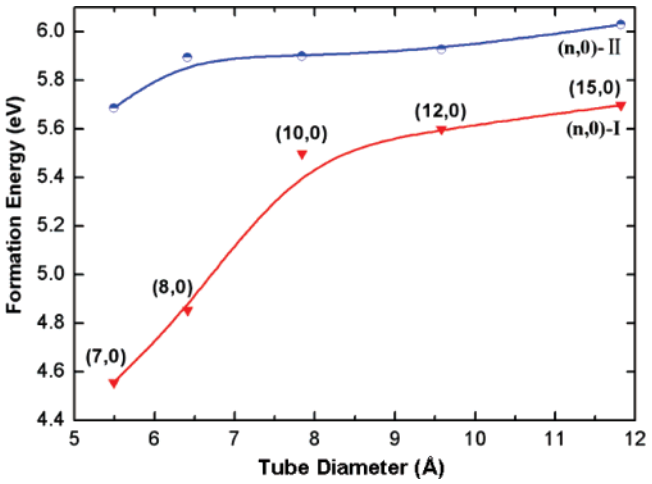

Figure 2. Energies of formation of SW defects as a function of the tube diameters.

TABLE 2: H_2 Addition Reaction Energies (in eV) on Corresponding Sites in the Perfect and Defective (8,0) BNNTs, as Labeled in Parts a−c of Figure 5[a]

reaction site	(8,0)	(8,0)-I	(8,0)-II
1	0.90 (0.00)	0.38 (−0.52)	1.24 (0.34)
2	1.06 (0.16)	−0.17 (−1.07)	−0.24 (−1.14)
3		−1.17 (−2.07)	−2.08 (−2.98)
4		0.75 (−0.15)	0.74 (−0.16)
5		0.38 (−0.52)	0.89 (−0.01)
6		0.88 (−0.02)	0.80 (−0.10)
7		0.78 (−0.12)	0.82 (−0.08)
8		0.72 (−0.18)	0.10 (−0.80)
9		0.58 (−0.32)	0.74 (−0.16)
10		0.90 (0.00)	1.09 (0.19)
11			1.17 (0.27)
12			−0.16 (−1.06)

[a] The relative energies given in parentheses are based on the energy of addition of two H's on top of adjacent B and N atoms parallel to the tube axis (site 1 of Figure 5a).

15) BNNTs. The defect formation energies, plotted as a function of the tube diameter in Figure 2, increase with increasing tube diameters for both kinds of SW defects. The smallest diameter (7,0)-I BNNT has the lowest SW defect formation energy (4.56 eV). When the diameters are the same, (*n*,0)-I BNNTs are always more favorable energetically than (*n*,0)-II tubes.

We employed a 6 × 6 BN graphene sheet supercell (36 B atoms and 36 N atoms) to model a BNNT with an infinitely large diameter. Our large computed SW defect formation energy (7.28 eV) underscores the difficulties in producing SW defects in large-diameter BNNTs. Theoretical results for SW defect formation in single-walled CNTs are similar.[17] The preference of forming SW defects in small diameter tubes as we discussed above is in contrast to that found by An et al.[22] based on cluster model computations. However, note that An et al. used the frustration energy (or defect formation energy) obtained in an antisite BN sheet[29] for comparison, in which the pentagon and heptagon ring strain effects are not included.

3.3. Band Structures of (8,0) BNNTs with SW Defects. The electronic band structures of perfect and defective (8,0) BNNTs (Figure 3) reveal typical wide band gap semiconductor behavior. The 3.66-eV band gap of (8,0) BNNTs is reasonably consistent with previous theoretical results.[10,30] Picozzi et al. reported that the semiconducting properties of (10,0) semiconducting single-walled CNTs were preserved after introduction of SW defects, and only a small reduction in the band gap occurred.[19d] The same trend is obtained by cluster model computations.[22] Our PBC results for defective (8,0)-I and (8,0)-II BNNTs were similar in that the wide band gap semiconductor character was retained. The formation of SW defects in (8,0) BNNTs leads to new levels at the top of the valence band and at the bottom of the conduction band. This reduces the BNNT band gaps by 0.21 and 0.47 eV for (8,0)-I and (8,0)-II, respectively.

The electron density isosurfaces of the top valence bands and bottom conduction bands of (8,0)-I and (8,0)-II tubes (Figure 4) clarify the origin of these new levels. The top valence bands originate mainly from the N atoms (especially those in N−N bonds) at the SW defect sites. Conversely, the B atoms of B−B bonds dominate the bottom conduction bands. Thus, the band gap reduction in these defective BNNTs is mainly due to the unfavorable N−N and B−B bonds in the SW defects.

Previous theoretical studies indicate that BN nanotubes have rather robust band structures: the electronic structures can only be modified slightly at low modification ratios by either addition reactions (such as fluorination,[10d] hydrogenation,[31] and amination[8]) or the presence of some native defects (such as antisites, carbon impurities, and vacancy defects[12,13]). This is reinforced

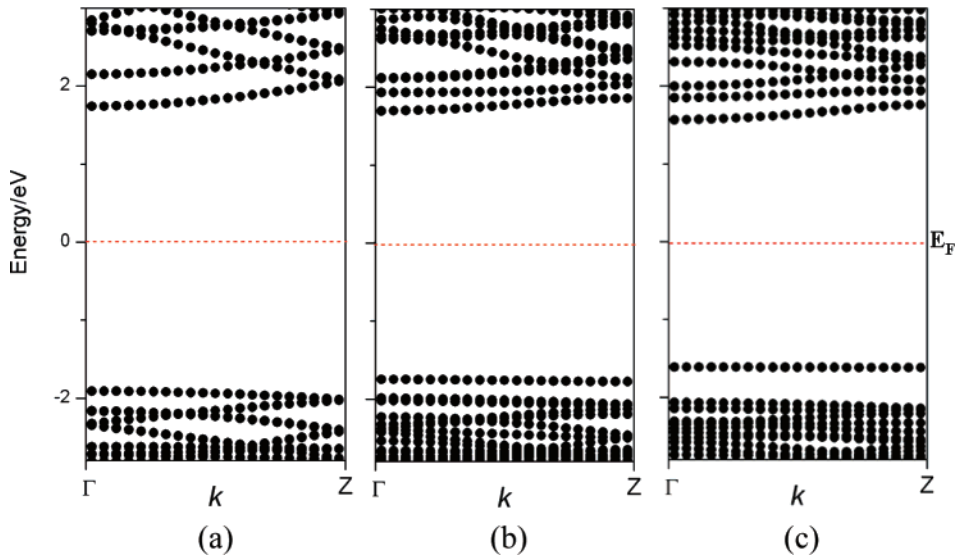

Figure 3. Band structures of (8,0) BNNTs: perfect (a) and defective (8,0)-I (b) or (8,0)-II (c) SW. Dashed lines indicate the Fermi level positions.

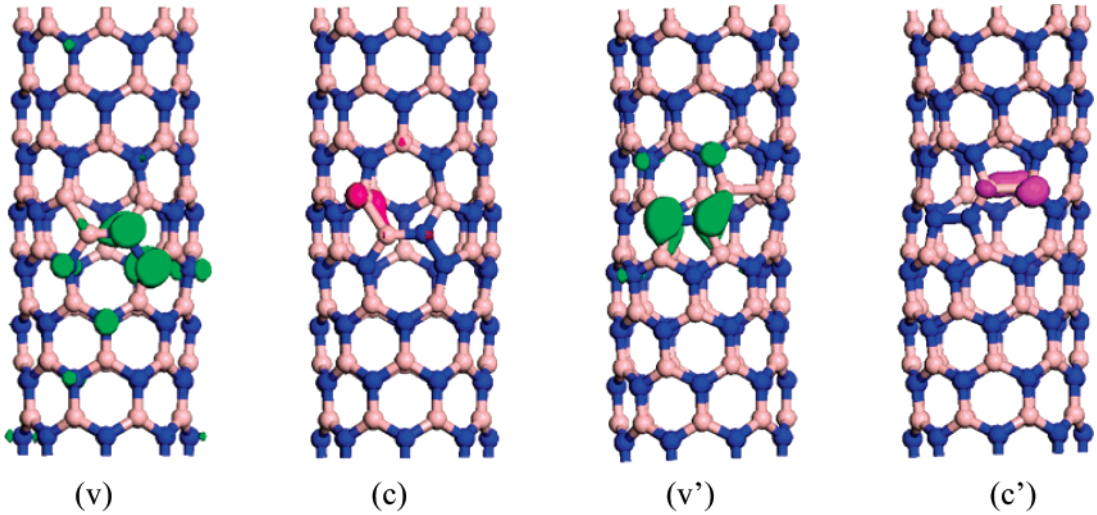

Figure 4. Electron density isosurfaces of the highest-energy valence (v and v') and of the lowest-energy conduction (c and c') bands (both mainly due to the SW defects) of (v)−(c) (8,0)-I, and (v')−(c') (8,0)-II.

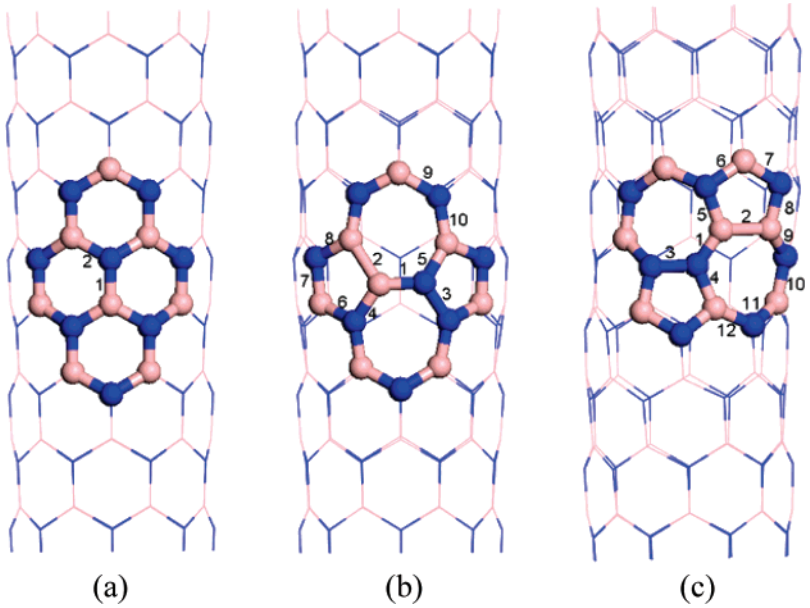

Figure 5. Schematic representation of possible sites for addition of two H's to (a) perfect (8,0) and (b) (8,0)-I or (c) (8,0)-II defective BNNTs.

by our computations on SW defective BN nanotubes and by additional computations on (8,0) BNNTs with hydrogen-terminated vacancies (see Supporting Information). Note that vacancies are unavoidable in the synthesis, and the dangling bonds of the vacant sites tend to be terminated due to their high reactivity. The sturdy electronic properties make BNNTs promising for many applications, especially in nanoelectronics.

3.4. Chemical Reactivity of SW Defects in (8,0) BNNTs. The chemical reactivity of SW defects in single-walled CNTs has been well studied. While SW defect sites were long believed to be more reactive than perfect sites,[17−19] Lu et al. reported recently that the central C−C bond of SW defects in an armchair (5,5) single-walled CNT is less reactive chemically than the C−C bonds at perfect sites. This behavior was attributed to the decrease of Θ_P of C atoms at the SW defects.[20] Our results in Table 1 reveal that the Θ_P's of atoms at both (8,0)-I and (8,0)-II SW defects vary appreciably. This will affect the chemical reactivity of SW defects since nanotube sidewall reactivity depends critically on the tube curvature.

We used hydrogenation reactions to probe the local chemical reactivity of SW defect sites in BNNTs. Characteristic sites related to the defects, such as 7-7, 6-7, 5-7, and 5-6 ring fusions, were considered. Possible hydrogenation sites on the sidewalls of perfect and defective (8,0) BNNTs are illustrated schematically in Figure 5.

Wu et al. found that two H's are best adsorbed on an outside wall of perfect zigzag BNNTs at adjacent B and N sites parallel to the tube axis.[6f] Our DFT results confirm their computations, but we stress that all addition reactions of H_2 are strongly endothermic. The energy of addition of two H's (of a H_2 molecule) on top of adjacent B and N atoms parallel to the tube axis of a perfect (8,0) BNNT (site 1 of Figure 5a) is (0.16 eV) less unfavorable than addition of two H's on top of adjacent B and N atoms slanted to the tube axis (site 2 of Figure 5a).

The energy (0.38 eV) of addition of H_2 to the B and N atoms at the 7-7 ring fusion of SW defects of (8,0)-I is less unfavorable than that (0.90 eV) at site 1 of the perfect (8,0) BNNT. In this sense, the chemical reactivity at this SW defect is better compared with perfect tubes. This result is consistent with Wu et al.'s theoretical study,[6h] but we stress that the common practice of basing reaction energies on fictitious H atom energies is unrealistic and grossly misleading. No hydrogen atoms are present in hydrogen gas, and 4.5 eV is required to dissociate H_2 into H atoms. Most of the SW-related (8,0)-I defect sites

are better than sites in perfect tubes (see Table 2) (although most of these are unfavorable thermodynamically). As the 7-7 ring fusion is perpendicular to the tube axis, it has more severe strain and, accordingly, is better than most of the 6-7 and 5-6 ring fusion sites. However, 7-7 ring fusion is not the most reactive site of SW defect of (8,0)-I. In the above sections, we have shown that the newly formed N−N bonds and B−B bonds are energetically unfavorable and that they contribute mainly to the top valence bands and the bottom conduction bands, respectively. Therefore, it is not surprising that the most reactive site of (8,0)-I is the N−N site (−1.17 eV) followed by B−B site (−0.17 eV). The (8,0)-II exhibits similar results due to the same reason. Two H's added to the N−N site (−2.08 eV) is the most exothermic for (8,0)-II and followed by that to the B−B site (−0.24 eV). Moreover, the B−B and N−N sites of (8,0)-II are completely perpendicular to the tube axis, which may explain the higher reactivity of these two sites than those of (8,0)-I. Like in (8,0)-I, most of the sites related to SW defect of (8,0)-II are less unfavorable than the sites in perfect tubes. However, when H_2 is added to the 7-7 ring fusion of SW defects in (8,0)-II, the computed reaction energy (1.24 eV) is more endothermic than those of either on the site 1 (0.90 eV) or on the site 2 (1.06 eV) of the perfect (8,0) BNNT. Among all the sites we studied for (8,0)-II (including 7-7, 6-7, 5-7, and 5-6 ring fusion), 7-7 ring fusion is the most endothermic, which is quite different from the (8,0)-I cases. The rather short bond length (1.361 Å) and the significant decrease of Θ_P of N atoms (from 9.15 to 2.54°) may be contributing to the greater endothermicity of these sites. Like the 7-7 ring fusion, addition to some 5-7 ring fusion sites are less endothermic than at the 6-7 ring fusion sites of (8,0)-I at SW defects (such as site 5 vs site 8). For (8,0)-II, H_2 addition to the 5-7 ring fusion (site 5) is more endothermic than that 6-7 ring fusion (site 8). This variation should be attributed to the different strain energies of these bonds with different orientations. Thus, the orientation of SW defects rather than the nature of ring fusions is the main influence on the addition energies. These results are similar to the findings for CNTs.[20]

4. Conclusion

SW defects in a series of zigzag (*n*,0) single-walled BNNTs were investigated by DFT computations. Two types of SW defects in each (*n*,0) BNNT, labeled as (*n*,0)-I and (*n*,0)-II, were considered. The former type is obtained by rotating the B−N bond parallel to tube axis, while the latter involves rotating a slanted B−N bond. SW defects induce structural deformation in BNNTs and change the local curvature at defect sites. The SW orientation determines the defect formation energies and the local structural distortion. SW defects form easily in small diameter BNNTs, and (*n*,0)-I defects are preferred energetically over (*n*,0)-II defects. The reactivity of SW defect BNNTs were probed by hydrogenation reactions. The energies of addition of two H's are mostly endothermic when these are based realistically on the energy of H_2 (rather than that of fictitious H atoms). Most of the SW defect sites are less endothermic than those in perfect tubes. Additions to the 7-7 ring fusion at SW defects (site 1 in Figure 5b and 5c) can be more or less endothermic than the perfect tube, depending on the SW defect orientations; the (8,0)-I SW defect is less, but the (8,0)-II defect is more endothermic than perfect BNNTs. The homoelement N−N bonds (site 3 in Figure 5b and 5c) are the most favorable SW defect sites in two defective (8,0) tubes, followed by the B−B bond sites (site 2 in Figure 5b and 5c), and both sites can react with molecular H_2 exothermically. The electronic structures can only be altered slightly by SW defects and by some other native defects (such as antisites, carbon impurities, and vacancy defects) and by addition reactions at low modification ratios. The robust band structures also make BNNTs promising for many applications, especially in nanoelectronics.

Acknowledgment. This study was supported in China by NSFC (50502021) and in the USA by NSF Grant CHE-0716718. Z.C. thanks the Special Coordination Funds for Promoting Science and Technology from the MEXT, Japan, to support his visit at the International Center for Young Scientists. We also thank Dr. Chengchun Tang, Dr. Chunyi Zhi and Dr. Wenlong Wang (NIMS, Tsukuba) for helpful discussions.

Supporting Information Available: The pyramidal angles of atoms close to the SW sites, optimized geometries, and band structures of (8,0) BNNTs with hydrogen-terminated vacancies. This material is available free of charge via the Internet at http://pubs.acs.org.

References and Notes

(1) For recent reviews, see: (a) Ma, R. Z.; Golberg, D.; Bando, Y.; Sasaki, T. *Philos. Trans. R. Soc. London, Ser. A* **2004**, *362*, 2161. (b) Terrones, M.; Romo-Herrera, J. M.; Cruz-Silva, E.; López-Urías, F.; Muñoz-Sandoval, E.; Velázquez-Salazar, J. J.; Terrones, H.; Bando, Y.; Golberg, D. *Mater. Today* **2007**, *10*, 30. (c) Golberg, D.; Bando, Y.; Tang, C. C.; Zhi, C. Y. *Adv. Mater.* **2007**, *19*, 2413.

(2) Rubio, A.; Corkill, J. L.; Cohen, M. L. *Phys. Rev. B* **1994**, *49*, 5081.

(3) Chopra, N. G.; Luyken, R. J.; Cherrey, K.; Crespi, V. H.; Cohen, M. L.; Louie, S. G.; Zettl, A. *Science* **1995**, *269*, 966.

(4) (a) Golberg, D.; Han, W.; Bando, Y.; Bourgeois, L.; Kurashima, K.; Sato, T. *Scipta Mater.* **2001**, *44*, 1561. (b) Chen, Y.; Zou, J.; Campbell, S. J.; Caer, G. L. *Appl. Phys. Lett.* **2004**, *84*, 2430.

(5) Yum, K.; Yu, M. F. *Nano Lett.* **2006**, *6*, 329.

(6) (a) Ma, R. Z.; Bando, Y.; Zhu, H. W.; Sato, T.; Xu, C. L.; Wu, D. H. *J. Am. Chem. Soc.* **2002**, *124*, 7672. (b) Tang, C. C.; Bando, Y.; Ding, X. X.; Qi, S. R.; Golberg, D. *J. Am. Chem. Soc.* **2002**, *124*, 14550. (c) Baierle, R. J.; Piquini, P.; Schmidt, T. M.; Fazzio, A. *J. Phys. Chem. B* **2006**, *110*, 21184. (d) Jhi, S. H.; Kwon, Y. K. *Phys. Rev. B* **2004**, *69*, 245407. (e) Zhou, Z.; Zhao, J. J.; Chen, Z.; Gao, X. P.; Yan, T. Y.; Schleyer, P.v.R. *J. Phys. Chem. B* **2006**, *110*, 13363. (f) Wu, X. J.; Yang, J. L.; Hou, J. G.; Zhu, Q. S. *J. Chem. Phys.* **2004**, *121*, 8481. (g) Wu, X. J.; Yang, J. L.; Hou, J. G.; Zhu, Q. S. *Phys. Rev. B* **2004**, *69*, 153411. (h) Wu, X. J.; Yang, J. L.; Hou, J. G.; Zhu, Q. S. *J. Chem. Phys.* **2006**, *124*, 54706. (i) Wu, X. J.; Yang, J. L.; Zeng, X. C. *J. Chem. Phys.* **2006**, *125*, 44704. (j) Durgun, E.; Jang, Y. R.; Ciraci, S. *Phys. Rev. B* **2007**, *76*, 073413.

(7) (a) Zhou, Z.; Zhao, J. J.; Gao, X. P.; Chen, Z.; Lu, J. P.; Schleyer, P.v.R.; Yang, C. K. *J. Phys. Chem. B* **2006**, *110*, 2529. (b) Yang, C. K.; Zhao, J. J.; Lu, J. P. *Phys. Rev. B* **2006**, *74*, 235445. (c) Xiang, H. J.; Yang, J. L.; Hou, J. G.; Zhu, Q. S. *New J. Phys.* **2005**, *7*, 39. (d) Zhang, Z. H.; Guo, W. L.; Tai, G. A. *Appl. Phys. Lett.* **2007**, *90*, 133103. (e) Shelimov, K. B.; Moskovits, M. *Chem. Mater.* **2000**, *12*, 250. (f) Zhou, Z.; Nagase, S. *J. Phys. Chem. C* **2007**, *111*, 18533.

(8) (a) Wu. X. J.; An, W.; Zeng, X. C. *J. Am. Chem. Soc.* **2006**, *128*, 12001. (b) Li, Y.; Zhou, Z.; Zhao, J. *J. Chem. Phys.* **2007**, *127*, 184705.

(9) (a) Zhi, C. Y.; Bando, Y.; Tang, C. C.; Golberg, D. *Phys. Rev. B* **2006**, *74*, 153413. (b) Li, Y.; Zhou, Z.; Zhao, J. *Nanotechnology* **2008**, *19*, 015202.

(10) (a) Tang, C. C.; Bando, Y.; Huang, Y.; Yue, S. L.; Gu, C. Z.; Xu, F. F.; Golberg, D. *J. Am. Chem. Soc.* **2005**, *127*, 6552. (b) Xiang, H. J.; Yang, J. L.; Hou, J. G.; Zhu, Q. S. *Appl. Phys. Lett.* **2005**, *87*, 243113. (c) Lai, L.; Song, W.; Lu, J.; Gao, Z.; Nagase, S.; Ni, M.; Mei, W.N.; Liu, J.; Yu, D.; Ye, H. *J. Phys. Chem. B* **2006**, *110*, 14092. (d) Zhou, Z.; Zhao, J. J.; Chen, Z.; Schleyer. P.v.R. *J. Phys. Chem. B* **2006**, *110*, 25678.

(11) Stone, A. J.; Wales, D. J. *Chem. Phys. Lett.* **1986**, *128*, 501.

(12) (a) Piquini, P.; Baierle, R. J.; Schmidt, T. M.; Fazzio, A. *Nanotechnology* **2005**, *16*, 827. (b) Schmidt, T. M.; Baierle, R. J.; Piquini, P.; Fazzio, A. *Phys. Rev. B* **2003**, *67*, 113407.

(13) Zobelli, A.; Ewels, C. P.; Gloter, A.; Seifert, G.; Stephan, O.; Csillag, S.; Colliex, C. *Nano Lett.* **2006**, *6*, 1955.

(14) Blasé, X.; De Vita, A.; Charlier, J. C.; Car, P. *Phys. Rev. Lett.* **1998**, *80*, 1666.

(15) Bettinger, H. F.; Dumitrica, T.; Scuseria, G. E.; Yakobson, B. I. *Phys. Rev. B* **2002.**, *65*, 041406.

(16) Miyamoto, Y.; Rubio, A.; Berber, S.; Yoon, M.; Tomanek, D. *Phys. Rev. B* **2004**, *69*, 121413.

(17) Pan, B. C.; Yang, W. S.; Yang, J. L. *Phys. Rev. B* **2000**, *62*, 12652.
(18) Grujicic, M.; Cao, G.; Rao, A. M.; Tritt, T.M.; Nayak, S. *Appl. Surf. Sci.* **2003**, *214*, 289.
(19) (a) Zhou, L. G.; Shi, S. Q. *Carbon* **2003**, *41*, 579. (b) Meng, F. Y.; Zhou, L. G.; Shi, S. Q.; Yang, R. *Carbon* **2003**, *41*, 2009. (c) Andzelm, J.; Govind, N.; Maiti, A. *Chem. Phys. Lett.* **2006**, *421*, 58. (d) Picozzi, S.; Santucci, S.; Lozzi, L.; Valentini, L.; Delley, B. *J. Chem. Phys.* **2004**, *120*, 7147.
(20) (a) Lu, X.; Chen, Z.; Schleyer, P.v.R. *J. Am. Chem. Soc.* **2006**, *128*, 12001. (b) Chakrapani, N.; Zhang, Y. M.; Nayak, S. K.; Moore, J. A.; Carroll, D. L.; Choi, Y. Y.; Ajayan, P. M. *J. Phys. Chem. B* **2003**, *107*, 9308. (c) Wang, C. C.; Zhou, G.; Liu, H. T.; Wu, J.; Qiu, Y.; Gu, B. L.; Duan, W. H. *J. Phys. Chem. B* **2006**, *110*, 10266. (d) Bettinger, H. F. *J. Phys. Chem. B* **2005**, *109*, 6922. (e) Dinadayalane, T. C.; Leszczynski, *J. Chem. Phys. Lett.* **2007**, *434*, 86.
(21) (a) Chandra, N.; Namilae, S.; Shet, C. *Phys. Rev. B* **2004**, *69*, 094101. (b) Ren, Y.; Xiao, T.; Liao, K. *Phys. Rev. B* **2006**, *74*, 045410.
(22) An, W.; Wu, X.; Yang, J. L.; Zeng, X. C. *J. Phys. Chem. C* **2007**, *111*, 14105.
(23) (a) Loiseau, A.; Willaime, F.; Demoncy, N.; Hug, G.; Pascard, H. *Phys. Rev. Lett.* **1996**, *76*, 4737. (b) Golberg, D.; Han, W.; Bando, Y.; Bourgeois, L.; Kurashima, K.; Sato, T. *J. Appl. Phys.* **1999**, *86*, 2364. (c) Menon, M.; Srivastava, D. *Chem. Phys. Lett.* **1999**, *307*, 407. (d) Arenal, R.; Kociak, M.; Loiseau, A.; Miller, D. J. *Appl. Phys. Lett.* **2006**, *89*, 073104.
(24) (a) Kresse, G.; Hafner, J. *Phys. Rev. B* **1993**, *47*, 558.(b) Kresse, G.; Hafner, J. *Phys. Rev. B* **1994**, *49*, 14 251. (c) Kresse, G.; Furthmüller, J. *Comput. Mat. Sci.* **1996**, *6*, 15. (d) Kresse, G.; Furthmüller, J. *Phys. Rev. B* **1996**, *54*, 11169.
(25) Perdew, J. P.; Chevary, J. A.; Vosko, S. H.; Jackson, K. A.; Pederson, M. R.; Singh, D. J.; Fiolhais, C. *Phys. Rev. B* **1992**, *46*, 6671.
(26) Vanderbilt, D. *Phys. Rev. B* **1990**, *41*, 7892.
(27) (a) Haddon, R. C.; Scott, L. *Pure Appl. Chem.* **1986**, *58*, 137. (b) Haddon, R. C. *J. Am. Chem. Soc.* **1986**, *108*, 2837. (c) Haddon, R. C. *J. Am. Chem. Soc.* **1987**, *109*, 1676. (d) Haddon, R. C. *J. Am. Chem. Soc.* **1990**, *112*, 3385. (e) Haddon, R. C. *Science* **1993**, *261*, 1545.
(28) Yang, S. H.; Shin, W. H.; Kang, J. K. *J. Chem. Phys.* **2006**, *125*, 084705.
(29) Charlier, J.-Ch.; Blase, X.; De Vita, A.; Car, R. *Appl. Phys. A* **1999**, *68*, 267.
(30) Xiang, H. J.; Yang, J. L.; Hou, J. G.; Zhu, Q. S. *Phys. Rev. B* **2003**, *68*, 035427.
(31) Zhang, J.; Loh, K. P.; Yang, S. W.; Wu, P. *Appl. Phys. Lett.* **2005**, *87*, 243105.